Chapter 3

Nuclear magnetic resonance

Introduction

The field of NMR began in 1946 with the independent and simultaneous work of two physics groups led by Edward Purcell and Felix Bloch (Bloch *et al.* 1946; Purcell *et al.* 1946). Building on earlier work in nuclear magnetism, these groups performed the first successful experiments demonstrating the phenomenon of NMR. Certain nuclei (including hydrogen) possess an intrinsic magnetic moment, and when placed in a magnetic field, they rotate with a frequency proportional to the field. This "delicate motion" first detected by Purcell and Bloch has proved to have far-reaching applications in fields they could hardly have imagined (see Box 3.1). In this chapter and the next, the basic concepts and techniques of MRI are described. In Chapter 5, the different approaches to fMRI are described, including contrast agent and arterial spin labeling techniques in addition to the intrinsic blood oxygenation level dependent (BOLD) signal changes introduced in earlier chapters. Because these techniques depend on subtle properties of the NMR signal, it is necessary to understand in some detail how MRI works.

Magnetic resonance imaging has become an indispensable tool in diagnostic radiology. It reveals fine details of anatomy, and yet is non-invasive and does not require ionizing radiation such as X-rays. It is a highly flexible technique so that contrast between one tissue and another in an image can be varied simply by varying the way the image is made. Figure 3.1 shows three MR images of the same anatomical section, exhibiting radically different patterns of contrast. These three images are described as T_1 weighted, density

Box 3.1. The historical development of NMR and MRI

A new tool for physics

In the early part of the twentieth century, it became clear that classical physics could not account for the world of atoms and subatomic particles. Experiments showed that the light emitted from excited atoms consisted of discrete frequencies, suggesting that only certain energy states could exist rather than a continuum of states. To explain subtle but distinct splittings of some of these spectral lines, called the hyperfine structure, Pauli proposed in 1924 that atomic nuclei possess an intrinsic angular momentum (*spin*) and an associated magnetic moment. The interaction of the electrons in the atom with the magnetic field of the nucleus creates a slight shift in the energy levels and a splitting of the spectral lines. The significance of these small effects is that they provide a window to investigate the basic properties of matter. From the magnitude of this hyperfine structure, one could estimate the magnitude of the nuclear magnetic moment, but the precision of these experiments was poor. In the 1930s, new techniques were developed based on the deflection of molecular beams in an inhomogeneous magnetic field (Bloch 1953), but these techniques were still inadequate for precision measurements.

The Second World War brought a stop to all basic physics research and perhaps explains the burst in creative activity just after the war that led to the seminal work of Purcell and Bloch. During the war, Purcell worked at the Massachusetts Institute of Technology on radar development and Bloch worked at Harvard on radar countermeasures, and their experience with RF techniques and measurements may have contributed to the success of their NMR studies (Vleck 1970). In fact, the experiments performed by Purcell and Bloch were rather different, but it was quickly realized that they were looking at two different aspects of the same phenomenon: in a magnetic field nuclei precess at a rate proportional to the field, with the spin axis rotating at a characteristic frequency. Purcell showed that electromagnetic energy is absorbed by a material at this resonant frequency, and Bloch showed that the precessing nuclei induce a detectable oscillating signal in a nearby detector coil. In both experiments, magnetic properties of the nucleus are manifested in terms of a frequency of electromagnetic oscillations, which can be measured with very high precision. In the next few years, NMR became a key tool for investigating atomic and nuclear properties based on these small effects of nuclear magnetization. In 1952, Purcell and Bloch were awarded the Nobel Prize in Physics for the development of NMR techniques and the contributions to basic physics made possible by NMR.

A new tool for chemistry

In Purcell's Nobel award lecture, quoted at the beginning of the chapter, he eloquently describes the feelings of a basic scientist who has discovered a previously unappreciated aspect of the world (Purcell 1953). At this time, NMR was valued as a tool for fundamental physics research, but the remarkable applications of NMR in other fields were still unimagined. In fact, much of the subsequent development of the field of NMR can be viewed as turning artifacts in the original techniques into powerful tools for measuring other properties of matter. The original application of NMR was to measure magnetic moments of nuclei based on their resonant frequencies. However, as experimenters moved up the periodic table to heavier atoms, it became clear that additional corrections were necessary to take into account shielding of the nucleus by atomic electrons. Electron orbitals create magnetic fields that alter the field felt by the nucleus, and the result is that the resonant frequency is shifted slightly depending on the chemical form of the nucleus.

In time, this chemical shift artifact in the nuclear magnetic moment measurements became the basis for applications of NMR in analytical chemistry, and NMR spectroscopy has now become an enormously powerful tool for chemical analysis. For example, the ^{1}H NMR spectrum of a sample of tissue from the brain is split into numerous lines corresponding to the different chemical forms of hydrogen. By far the most dominant line is from water, but if this strong signal is suppressed, many

other lines appear. Although the frequency differences are small, only a few parts per million, they are nevertheless readily measurable. The relative intensities of the different lines directly reflect the proportion of the corresponding chemical in the sample. A key development in the methodology used in these chemistry applications was the introduction by Richard Ernst of Fourier methods for acquiring and analyzing the signal. Rather than sweeping the magnetic field to excite each spectral line in turn, all of the nuclei are excited at once and the spectrum is sorted out from the combined signals using the Fourier transform. This same basic methodology has carried through to current MRI methods. In 1991, Ernst received the Nobel Prize in Chemistry for his work in applications of NMR to basic chemistry studies.

A new tool for medicine

Because the resonant frequency of a nucleus is directly proportional to the magnetic field, any inhomogeneities of the magnet translate into an unwanted broadening of the spectral lines. In 1973, Paul Lauterbur proposed that NMR techniques could also be used for imaging by deliberately altering the magnetic field homogeneity in a controlled way. By applying a linear gradient field to a sample, the NMR signals from different locations are spread out in frequency, analogous to the way that the signals from different chemical forms of the nucleus are spread in frequency. Measuring the distribution of frequencies in the presence of a field gradient then provides a direct measure of the distribution of signals within the sample: an image. Peter Mansfield (1977) showed how rapid switching of gradients makes possible fast imaging with a technique called echo-planar imaging (EPI). The first commercial MR imagers were built in the early 1980s, and MRI is now an essential part of clinical radiology. In 2003, Lauterbur and Mansfield were awarded the Nobel Prize in Physiology or Medicine for their contributions to the development of MRI.

A new tool for mapping brain activity

Even with a perfectly homogeneous magnet, the heterogeneity of the human body itself leads to local variations in the magnetic field. These field inhomogeneities first appeared in images as artifacts, either a distortion of the image or a reduction of the local signal because nuclear spins precessing at different rates become out of phase with each other, reducing the net signal. In the early 1990s, it was demonstrated that the oxygenation state of hemoglobin has a measurable effect on the signal measured with MRI (Ogawa *et al.* 1990), and this soon led to the capability of mapping brain activity based on blood oxygenation changes accompanying neural activation (Kwong *et al.* 1992). This technique of fMRI has become a standard tool for functional neuroimaging and is now widely used for mapping the working human brain.

weighted, and T_2 weighted (the meaning of these technical terms will be made clear shortly). The source of the flexibility of MRI lies in the fact that the measured signal depends on several properties of the tissue, as suggested by these descriptions. This is distinctly different from other types of radiological imaging. For example, in computed tomography (CT) the image is a map of one local property of the tissue: the X-ray absorption coefficient. Similarly, with nuclear medicine studies, the image is a map of the radioactive tracer concentration. But with MRI, the image is a map of *the local transverse magnetization of the hydrogen nuclei*. This transverse magnetization, in turn, depends on several intrinsic properties of the tissue. In fact, the transverse magnetization is a transient phenomenon; it does not exist until we start the MRI process.

The fact that the MR signal depends on a number of tissue properties is the source of its flexibility, but it is also a source of difficulty in developing a solid grasp of MRI. To

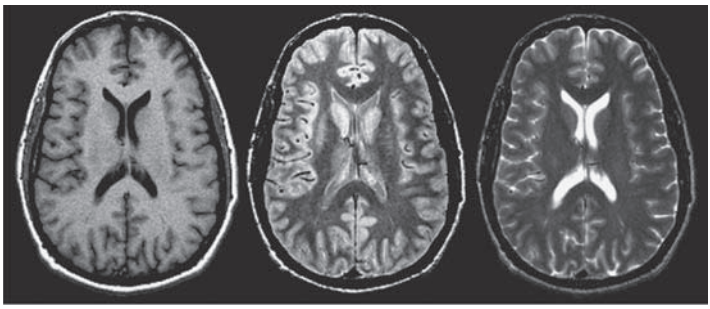

Fig. 3.1. Magnetic resonance images of the same anatomical section showing a range of tissue contrasts. In the first image, cerebrospinal fluid is black, whereas in the last image it is bright. Contrast is manipulated during image acquisition by adjusting several parameters, such as the repetition time TR and the echo time TE (times given in milliseconds), which control the sensitivity of the signal to the local tissue relaxation times T_1 and T_2 and the local proton density.

understand the full range of MRI applications, it is necessary to understand the basic physics of NMR and how the MR signal can be manipulated experimentally.

The NMR signal

The basic NMR experiment

The phenomenon of NMR is not part of everyday experience, so it is helpful to set the stage by considering a purely empirical description of the basic experiment. Every time an MR image is made, it is a variation on this basic experiment. For the moment we are only concerned with how the MR signal is generated; how that signal is mapped to create an image is taken up in Chapter 4. The basic experimental setup is illustrated in Fig. 3.2. A sample is placed in a large magnetic field, and a coil of wire is placed near the sample oriented such that the axis of the coil is perpendicular to the magnetic field. The coil is used as both a transmitter and a receiver. During the *transmit* phase of the experiment, an oscillating current is applied to the coil for a brief time (a few milliseconds), which produces an oscillating magnetic field in the sample. The oscillations are in the radiofrequency (RF) range, so the coil is often referred to as an *RF coil*, and the brief oscillating magnetic field is referred to as an *RF pulse*. For example, for clinical imaging systems with a magnetic field of 1.5 tesla (1.5 T; about 30 000 times stronger than the natural magnetic field at the surface of the earth), the oscillating field has a magnitude of only a few microtesla, and the oscillations are at a frequency of 64 MHz. During the receive phase of the experiment, the coil is connected to a detector circuit that senses small oscillating currents in the coil.

The basic experiment consists of applying a brief RF pulse to the sample and then monitoring the current in the coil to see if there is a signal returned from the sample. If one were to try this experiment naively, with an arbitrary RF frequency, the result would usually be that there is no returned signal. However, for a few specific frequencies there would be a weak, transient oscillating current detected in the coil. This current, oscillating at the same frequency as the RF pulse, is the NMR signal. The particular frequencies where it occurs are the resonant frequencies of particular nuclei. At its resonant frequency a nucleus is able to absorb electromagnetic energy from the RF pulse during the transmit phase and return a small portion of that energy back to the coil during the receive phase. Only particular

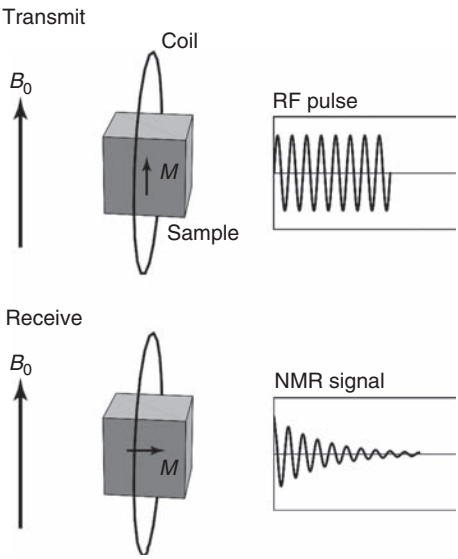

Fig. 3.2. The basic NMR experiment. A sample is placed in a large magnetic field B_0, and hydrogen nuclei partially align with the field creating a net magnetization M. In the transmit part of the experiment, an oscillating current in a nearby coil creates an oscillating radiofrequency (RF) magnetic field in the sample, which causes M to tip over and precess around B_0. In the receive part of the experiment, the precessing magnetization creates a transient oscillating current (the NMR signal) in the coil.

nuclei, those with an odd number of either neutrons or protons, exhibit NMR. For example, carbon-12 (^{12}C) with six protons and six neutrons does not show the NMR effect, whereas carbon-13 (^{13}C) with seven neutrons does have a resonance. In MRI studies, the nucleus of interest is almost always hydrogen.

As an analogy to the NMR experiment, imagine that we are sitting in a quiet room and have a tuning fork with a precise resonant frequency. Our "coil" is a speaker/microphone that can be used either for broadcasting a pure tone into the room or listening for a weak tone coming back from the room. For most frequencies broadcast into the room, there will be no return signal because the tuning fork is unaffected. But when the broadcast frequency matches the resonant frequency of the tuning fork, the fork will begin to vibrate, absorbing acoustic energy. Afterward, the microphone will pick up a weak sound coming back from the vibrating tuning fork.

Precession

The source of the resonance in an NMR experiment is that the protons and neutrons that make up a nucleus possess an intrinsic angular momentum called *spin*. The word spin immediately brings to mind examples of our classical concept of angular momentum: spinning tops, the spin of a curving baseball, and planets spinning on their axes. However, the physical concept of nuclear spin is a purely quantum mechanical phenomenon and is fundamentally different from these classical examples. For a spinning top, the "spin" is not an intrinsic feature of the top. The top can be spun faster or slower or stopped altogether. But for a proton, angular momentum is an intrinsic part of being a proton. All protons, neutrons, and electrons have the same magnitude of angular momentum, and it cannot be increased or decreased. The only feature that can change is the *axis of spin*, the direction of the angular momentum. When protons combine to form a nucleus, they combine in pairs with oppositely oriented spins, and neutrons behave similarly. The result is that nuclei with an even number of protons and an even number of neutrons, such as ^{12}C, have no net spin, whereas nuclei with an odd number, such as ^{13}C, do have a net spin. Hydrogen, with only a single

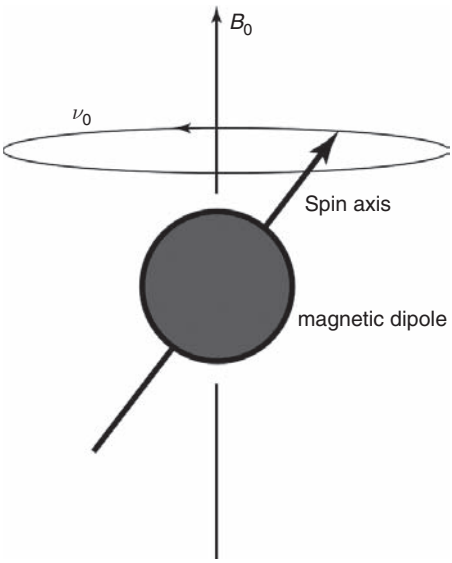

Fig. 3.3. Precession of a magnetic dipole in a magnetic field. The magnetic field B_0 exerts a torque on a nuclear magnetic dipole that would tend to make it align with B_0. However, because the nucleus also has angular momentum (spin), it instead precesses like a spinning top at an angle to the gravitational field. The precession frequency ν_0 is proportional to the magnetic field and is the resonant frequency of NMR.

proton as its nucleus, has a net spin, and because it is far more abundant in the body than any other nucleus, it is the primary focus of MRI.

Associated with the spin of the proton is a *magnetic dipole moment*. That is, the H nucleus behaves like a tiny magnet, with the north–south axis parallel to the spin axis. Now consider a proton placed in a magnetic field. Because of its magnetic dipole moment, the magnetic field exerts a torque on the proton that, in the absence of other effects, would rotate the dipole into alignment with the field, like a compass needle in the earth's magnetic field. But because the proton also possesses angular momentum, this alignment does not happen immediately. Instead, the spin axis of the proton *precesses* around the field axis rather than aligning with it (Fig. 3.3). This is an example of the peculiar nature of angular momentum: if one tries to twist a spinning object, the change in the spin axis is at right angles to both the original spin axis and the twisting axis. For example, the wheel of a moving bicycle has an angular momentum around a horizontal axis perpendicular to the bike. If the bike starts to tip to the left it can be righted by twisting the handle bars to the left. That is, applying a torque around a vertical axis (twisting the handle bars) causes the wheel to rotate around a horizontal axis along the length of the bike.

A more direct analogy is a spinning top whose axis is tilted from the vertical. Gravity applies a torque that would tend to make the top fall over. But instead the top precesses around the vertical, maintaining a constant tip angle. In thinking about this process, we must be clear about the distinction between the direction of the field and the axis of the torque the field creates. The gravitational field is vertical, but the torque it creates is around a horizontal axis because it would tend to rotate the top away from vertical, pivoting around the point of contact with the table.

Thus, when placed in a magnetic field, a proton with its magnetic dipole moment precesses around the field axis. The frequency of this precession, ν_0, is the resonant frequency of NMR, and is often called the Larmor frequency after the nineteenth century physicist who investigated the classical physics of precession in a magnetic field. The precession frequency is

Table 3.1. The gyromagnetic ratio for selected nuclei

Nucleus	Gyromagnetic ratio (MHz/T)
^{1}H	42.58
^{13}C	10.71
^{19}F	40.08
^{23}Na	11.27
^{31}P	17.25

directly proportional to the strength of the magnetic field because the torque applied to the dipole is proportional to the field. The fundamental equation of magnetic resonance is then

$$v_0 = \gamma B_0 \tag{3.1}$$

where B_0 is the main magnetic field strength and γ is a constant called the gyromagnetic ratio. The factor γ is different for each nucleus and is usually expressed in units of megahertz per tesla (Table 3.1). Equation (3.1) is the fundamental basis of MRI, which uses subtle manipulations of the resonant frequency to map the location of the signal.

Relaxation

The second important process that affects the orientation of the proton's spin in addition to precession is *relaxation*. If we place a proton in a large magnetic field, the precession rate is very fast: $\nu_0 = 64$ MHz in a 1.5 T field. If we could observe the angle of the dipole axis for a few rotations, we would see no change; it would appear as a pure precession with no apparent tendency for the dipole to align with the field. But if we observed the precession for millions of cycles, we would see that the dipole gradually tends to align with the magnetic field. The time constant for this relaxation process is called T_1, and after a time several times longer than T_1 the dipole is essentially aligned with B_0.

Relaxation is an example of energy equilibration. A dipole in a magnetic field is at its lowest energy when it is aligned with the field and at its highest energy when it is aligned opposite to the field. As the dipole changes orientation from its initial angle to alignment with the field, this orientational magnetic energy must be converted into other forms of energy, such as the random thermal motions of the molecules. In other words, the initial orientational magnetic energy must be dissipated as heat. The time required for this energy equilibration depends on how tightly coupled the random thermal motions are to the orientation of the dipole. For H nuclei in water molecules, this coupling is very weak, so T_1 is long. A typical value for T_1 in the human body is approximately 1 s, eight orders of magnitude longer than the precession period in a 1.5 T magnet.

Equilibrium magnetization

Now consider a collection of magnetic dipoles, a sample of water, in a magnetic field. Each H nucleus is a magnetic dipole; the oxygen nucleus (^{16}O) contains an even number of protons and neutrons and so has no net angular momentum nor a net magnetic moment. The spin axes of the individual H nuclei precess around the field, and over time they tend to align with the field. However, this alignment is far from complete. Exchanges of energy between the orientation of the dipole and thermal motions prevent the dipoles from settling into their

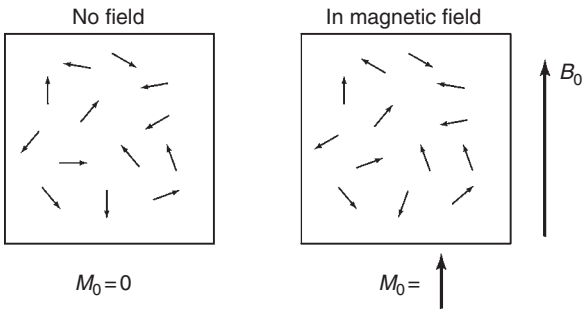

Fig. 3.4. Formation of an equilibrium magnetization (M_0) as a result of partial alignment of nuclear magnetic dipoles. In the absence of a magnetic field, the spins are randomly oriented, and there is no net magnetization. When placed in a magnetic field B_0, the spins partly align with the field, a relaxation process with a time constant T_1 of approximately 1 s, creating a net local magnetization.

lowest energy state. In fact, the energy difference between an H nucleus aligned with the field and one opposed to the field at 1.5 T is only approximately 1% of the random thermal energy of the water molecule. The result is that at equilibrium the difference between the number of spins aligned with the field and the number opposed to the field is only approximately 1 part in 10^5. Nevertheless, this creates a weak *equilibrium magnetization* M_0 aligned with the field (Fig. 3.4). The term M_0 is the net dipole moment per cubic centimeter, and one can think of it loosely as a weak, but macroscopic, local magnetic field that is the net result of summing up the magnetic fields of each of the H nuclei. That is, each cubic centimeter of a uniformly magnetized sample carries a net dipole moment M_0. The magnitude of M_0 is directly proportional to the local *proton density* (or *spin density*).

The radiofrequency pulse

The local value of M_0 is the net difference between dipoles aligned with the field and opposite to the field, but it is not directly observable because it is many orders of magnitude weaker than B_0. However, if all the dipoles that contribute to M_0 could be tipped 90°, they would all precess around the field at the same rate. Thus, M_0 would also tip 90° and begin to precess around the main field. Tipping over the magnetization produces a measurable, transient signal, and the tipping is accomplished by the RF pulse. During the transmit part of the basic NMR experiment, the oscillating RF current in the coil creates in the sample an oscillating magnetic field B_1 perpendicular to B_0. The field B_1 is in general several orders of magnitude smaller than B_0. Nevertheless, this causes the net magnetic field, the vector sum of B_1 and B_0, to wobble slightly around the B_0 direction. Initially M_0 is aligned with B_0, but when the net field is tipped slightly away from B_0, M_0 begins to precess around the new net field. If the oscillation frequency of B_1 is different from the precession frequency ν_0, not much happens to M_0 except a little wobbling around B_0. But if the RF frequency matches the precession frequency, a resonance phenomenon occurs. As the net magnetic field wobbles back and forth, the magnetization precesses around it in synchrony. The effect is that with each precessional rotation M_0 tips farther away from B_0, tracing out a growing spiral (Fig. 3.5). After a time, the RF field is turned off, and M_0 then continues to precess around B_0. The net effect of the RF pulse is thus to tip M_0 away from B_0, and such pulses are usually described by the *flip angle* they produce (e.g., a 90° pulse or a 30° pulse). The flip angle can be increased either by increasing the amplitude of B_1 or by leaving B_1 on for a longer time.

It is remarkable that a magnetic field as weak as B_1 can produce arbitrarily large flip angles. From an energetic point of view, tipping the net magnetization away from B_0 increases the orientational energy of the dipoles: the nuclei absorb energy from the RF

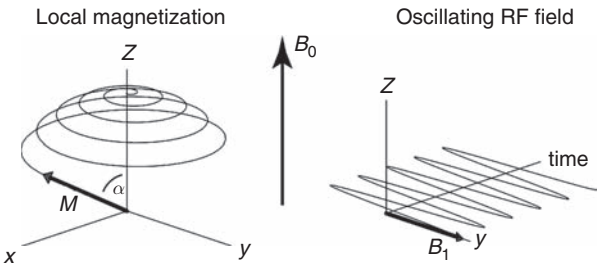

Fig. 3.5. Tipping over the magnetization with excitation by a radiofrequency (RF) pulse. The RF pulse is a small oscillating field B_1 perpendicular to B_0 that causes the net magnetic field to wobble slightly around the z-axis. As the magnetization M precesses around the net field, it traces out a widening spiral. It is tipped away from the longitudinal axis, and the final tip angle (or flip angle) α is controlled by the strength and duration of the RF pulse.

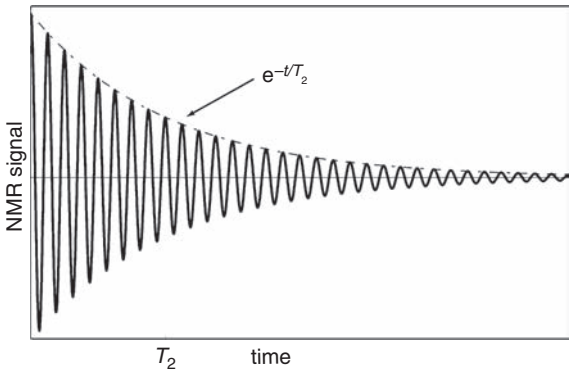

Fig. 3.6. Free induction decay. After a 90° radiofrequency pulse tips the longitudinal magnetization into the transverse plane, a detector coil measures an oscillating signal, which decays in amplitude with a time constant T_2 in a perfectly homogeneous magnetic field. (In an inhomogeneous field, the signal decays more quickly, with a time constant $T_2^* < T_2$.) The plot is not to scale; typically the signal will oscillate more than a million times during the interval T_2.

pulse. This transfer of energy is possible even with small B_0 fields because B_0 oscillates at the resonant frequency of the nuclei, the precession frequency. This is much like pushing a child on a swing. The swing has a natural resonant frequency, and giving very small pushes at that frequency produces a large amplitude of motion. That is, the swing efficiently absorbs the energy provided by the pusher when it is applied at the resonant frequency.

The free induction decay signal

A precessing macroscopic magnetization produces a magnetic field that is changing with time. This will induce a current in a nearby coil, creating a measurable NMR signal that is proportional to the magnitude of the precessing magnetization. This detected signal is called a *free induction decay* (FID) and is illustrated in Fig. 3.6. *Free* refers to free precession of the nuclei; *induction* is the electromagnetic process by which a changing magnetic field induces a current in the coil, and *decay* describes the fact that the signal is transient. The signal decays away because the precessing component of the magnetization itself decays away. The reason for this is that the individual dipoles that sum to produce the magnetization are not precessing at precisely the same rate. As a water molecule tumbles from thermal motions, each H nucleus feels a small, randomly varying magnetic field in addition to B_0 primarily from the other H nucleus in the molecule. When the random field adds to B_0, the dipole precesses a little faster, and when it subtracts from B_0, it precesses a little slower. For each nucleus, the pattern of random fields is different, so as time goes on the dipoles get progressively more out of phase with one another, and as a result no longer add coherently. The net precessing magnetization then decays away exponentially, and the time constant for this decay is called T_2.

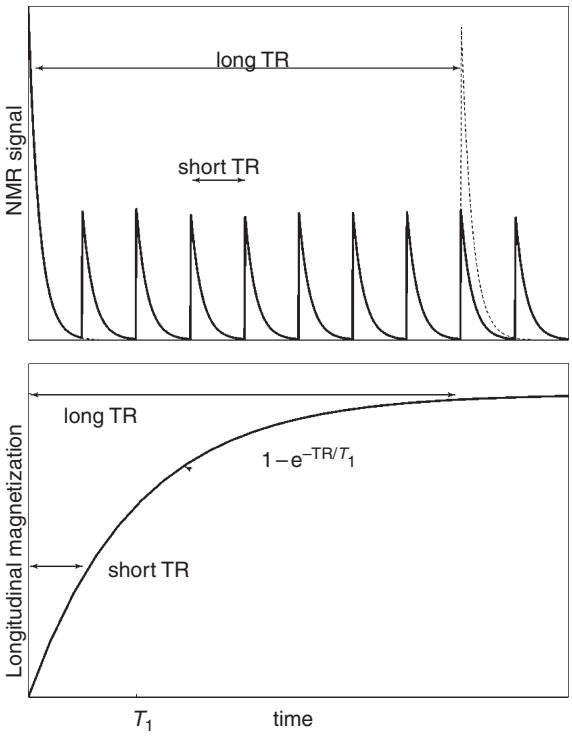

Fig. 3.7. Effect of repetition time (TR). Repeated radiofrequency (RF) pulses generate repeated free induction decay (FID) signals, but if TR is short, each repeated signal will be weaker than the first (top). The magnitude of the signal with a 90° RF pulse, is proportional to the magnitude of the longitudinal magnetization just prior to the RF pulse. After a 90° RF pulse, the longitudinal magnetization recovers toward equilibrium with a relaxation time T_1 (bottom). If this recovery is incomplete because TR < T_1, the next FID signal is reduced.

For the human brain at a magnetic field strength of 1.5 T, some approximate characteristic values for T_2 are 70 ms for white matter, 90 ms for gray matter, and 400 ms for cerebrospinal fluid (CSF). From this we can begin to see how tissue contrast can be produced in an MR image. By delaying measurement of the signal for 100 ms or so, the CSF signal will be much larger than the brain parenchyma signal, and an image of the signal distribution at that time will show CSF as bright and the rest of the brain as dark. The image on the right in Fig. 3.1 is an example of such a T_2*-weighted image*.

Now imagine repeating the experiment, after the signal has decayed away, to generate a new signal. How does this new signal compare with the first? The answer depends on the time between RF pulses, called the *repetition time* (TR). When TR is very long (say 20 s), the signal generated by the second RF pulse is equal in magnitude to that generated by the first RF pulse. As TR is shortened, the signal generated by the second RF pulse becomes weaker (Fig. 3.7). To generate a second full-amplitude signal, a recovery time of several times longer than T_1 is required to allow the spins to relax back to equilibrium. The recovery process is also exponential, described by the time constant T_1. This relaxation time also varies among tissues: at a magnetic field of 1.5 T, T_1 is approximately 700 ms for white matter, 900 ms for gray matter, and 4000 ms for CSF. Here we can see another way to produce contrast between tissues in an MR image. If the repetition time is short (say, TR = 600 ms), the signal from white matter will recover more fully than that of CSF, so white matter will appear bright and CSF dark in an image, as illustrated in the image on the left in Fig. 3.1. This is described as a T_1*-weighted image*.

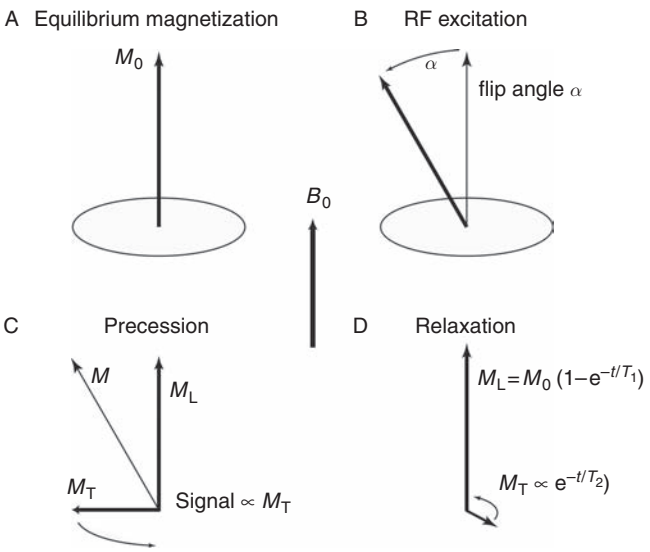

Fig. 3.8. The basic physics of the NMR experiment. (A) In a magnetic field B_0, an equilibrium magnetization M_0 forms from the alignment of nuclear dipoles (B.C). A radiofrequency (RF) pulse tips over M_0 (B), creating a longitudinal component M_L and a transverse component M_T (C). Then, M_T precesses around the direction of B_0, generating a detectable NMR signal. (D) Over time, M_T decays to zero with a relaxation time T_2 and M_L recovers to M_0 with a relaxation time T_1.

The basic NMR experiment again

We can now return to the basic NMR experiment and describe it in terms of the basic physics (Fig. 3.8). A sample of water is placed in a magnetic field B_0. Over an interval of time several times longer than T_1, the magnetic dipole moments of the H nuclei tend to align with B_0, creating a local macroscopic M_0 aligned with B_0. An RF pulse is applied that tips M_0 away from B_0, creating a transverse magnetization M_T. The newly created transverse magnetization precesses around B_0, generating a detectable signal in the coil (the FID) with an amplitude proportional to M_T. Over time, the precessing magnetization, and, therefore, the signal, decreases exponentially, and after a time several times longer than T_2 the signal is essentially gone. Meanwhile, the longitudinal magnetization along B_0 slowly re-forms, so that after several T_1 times we are back to where we started, with M_0 aligned with B_0.

However, if another RF pulse is applied before this recovery is complete, the longitudinal magnetization will be less than M_0. When this partially recovered magnetization is tipped over, M_T will be smaller, and, therefore, the detected MR signal will also be smaller. Again, the longitudinal magnetization re-grows from zero, and if another RF pulse is applied after the same interval TR, another FID will be created. However, if the RF flip angle is 90°, the amount of recovery during each successive TR period is the same: the longitudinal magnetization is reduced to zero after each 90° pulse and then relaxes for a time TR before the next RF pulse. So the signal generated after each subsequent RF pulse is the same as that after the second pulse. This signal, regenerated with each RF pulse, is described as the steady-state signal.

Nearly all MR imaging applications involve applying a series of RF pulses at a fixed repetition time, so the steady-state signal typically is measured. In fact, the signals from the first few pulses are usually discarded to allow the magnetization to reach a steady state. In this example with 90° pulses, the steady state is reached after one RF pulse, but for other flip angles several pulses are necessary. Thus, M_0 determines the maximum signal that can be generated; however, unless TR is much longer than T_1, the measured steady-state signal is less than this maximum.

A quantitative description of the MR signal produced by a particular tissue will, therefore, depend on at least three intrinsic tissue parameters: the proton density, which determines M_0, and the relaxation times T_1 and T_2. Note that for each of the brain tissues, T_1 is on the order of 10 times larger than T_2, which is usually the case with biological specimens. This means that the processes that lead to recovery are much slower than those that lead to signal decay.

We have just described a simple *pulse sequence*: an RF pulse is applied to the sample, and after a repetition time TR the same RF pulse is applied again. The signal generated after the second pulse depends on a pulse sequence parameter (TR) but also on properties of the sample (e.g., T_1). This basic theme runs throughout MRI. A particular pulse sequence will involve several parameters that can be adjusted in making the image, and these parameters interact with intrinsic parameters of the tissue to affect the measured signal. This dependence of the signal on multiple parameters gives MRI its unique flexibility.

At this point, it is helpful to review some of the standard terminology used in NMR. We are always dealing with a local three-dimensional magnetization vector $\boldsymbol{M}$. This is taken to have a *longitudinal* component parallel to B_0 and a *transverse* component perpendicular to B_0. The longitudinal axis is usually designated z, and the transverse plane is then the x–y plane. The *transverse* component of M (M_{xy} or M_T) is the part that precesses, so the detected signal is always proportional to the transverse component. The transverse component decays away with a time constant T_2, called the *transverse relaxation time*. At equilibrium the longitudinal magnetization has the value M_0, and there is no M_T. The time constant for the longitudinal magnetization to grow to its equilibrium value is T_1, *the longitudinal relaxation time*.

Basic pulse sequences

Pulse sequence parameters and image contrast

In the preceding sections, we considered how an MR signal is generated in a small volume of tissue. In MRI, the intensity of each pixel in the image is directly proportional to this local MR signal. That is, every MR image is a picture of the local value for M_T at the time the image data were collected. And because M_T is intrinsically a transient phenomenon, each MR image is a snapshot of a dynamic process at a particular time. Indeed, before the first excitation pulse there is no M_T at all, and the RF pulse sequence itself creates the quantity that is imaged. The MR signal depends on several intrinsic properties of the tissue (proton density and tissue relaxation times) and also on particular parameters of the pulse sequence used (e.g., TR). The power and flexibility of MRI derives from the fact that many pulse sequences are possible, and by adjusting pulse sequence parameters such as TR, the sensitivity of the MR signal to different tissue parameters can be adjusted to alter contrast in the image. For example, when TR is longer than any of the tissue T_1 values, each local magnetization recovers completely between RF pulses, so the local magnetization is insensitive to the local T_1. But if TR is shorter than the tissue T_1 values, recovery is incomplete, and the local magnetization depends strongly on the local T_1, creating a T_1-weighted signal.

At first glance, it might appear that the optimal choice of pulse sequence parameters would be those that maximize the signal. The MR signal is intrinsically weak, and noise in the images is the essential limitation on spatial resolution. In fact, maximum signal to noise ratio is not optimal for anatomical imaging as an image at such a ratio would be uniformly gray and not of much use. Instead, the contrast to noise ratio is what determines whether one tissue can be distinguished from another in the image. It is often useful for comparing

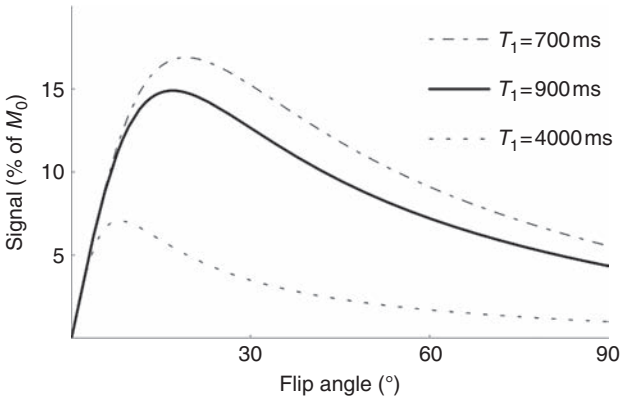

Fig. 3.9. Gradient recalled echo (GRE) signal. The dependence of the signal on flip angle for a spoiled GRE pulse sequence is illustrated for three values of T_1. For small flip angles, the signal is insensitive to T_1 (density weighted), but it is strongly T_1 weighted for larger flip angles. The flip angle for peak signal is substantially smaller than 90° and depends on T_1.

different pulse sequences to evaluate the contrast to noise ratio between standard tissues such as gray matter, white matter, and CSF. In the following section, we will consider the most commonly used pulse sequences and how they generate image contrast.

Gradient echo pulse sequence

The simplest pulse sequence is the free induction decay described above: a series of RF pulses creates a precessing M_T and a measurable signal. When an FID pulse sequence is used for imaging, it is called a *gradient recalled echo (GRE) pulse sequence*, for reasons that will be explained in Ch. 4. In its basic form, the pulse sequence depends on just two parameters: TR and the flip angle α. The strength of the signal depends on a combination of these adjustable parameters and the intrinsic tissue parameters S_0, the proton density, and T_1. (If the signal is measured soon after the RF pulse, there will be little time for the signal to decay away, and so it will not depend strongly on T_2.) The local MR signal is always proportional to the proton density because the proton density determines M_0 and thus sets the maximum value for M_T that could be produced. If TR is much longer than T_1, the longitudinal magnetization will fully recover during TR. Because the signal does not depend on T_1, but only on the proton density (M_0), the contrast with such a pulse sequence is described as density weighted. The fraction of the longitudinal magnetization that is tipped into the transverse plane is $\sin\alpha$, so a 90° RF pulse puts all the magnetization into the transverse plane and generates the largest signal. Therefore, for long TR the signal is density weighted and proportional to $\sin\alpha$.

However, with shorter TR values, the signal depends on TR, T_1, and α in a more interesting way (Fig. 3.9). In fact, the signal and contrast characteristics depend on precisely how the pulse sequence is constructed, which is discussed in Ch. 6. In anticipation of the terminology introduced there, the following discussion applies to a *spoiled GRE pulse sequence*. With $\alpha = 90°$, all the longitudinal magnetization is tipped over on each pulse, and there is little time for it to recover before the next pulse if TR $< T_1$. As a result, the steady-state magnetization created after each RF pulse is weak. The degree of recovery during TR depends strongly on T_1, so the resulting signal is strongly T_1 weighted. Note that the signal is still proportional to M_0, and so is also density weighted, but the popular terminology is to describe such a pulse sequence as simply T_1 weighted. However, the density weighting is important for determining tissue contrast. For most tissues in the body, a larger proton density is associated with a longer T_1, and this produces an essential conflict for achieving a good contrast to noise ratio between tissues: the density weighting would tend to

make the tissue with the larger T_1 brighter, but the T_1 weighting would tend to make the same tissue darker because there is less recovery for a longer T_1. The two sources of contrast thus conflict with each other. Nevertheless, T_1-weighted imaging is very common because the variability of T_1 between tissues is much greater than the variability of proton density, and so T_1 weighting usually dominates the contrast.

Alternatively, to produce a proton density-weighted image, the sensitivity to T_1 must be reduced. As already discussed, this can be done simply by using a long TR so that tissues with different T_1 values all recover to their equilibrium values. But a long TR is a disadvantage in conventional MRI. To collect sufficient data to reconstruct an image, the pulse sequence usually must be repeated many times, and so the total imaging time is proportional to TR. With a GRE pulse sequence there is another, somewhat surprising, way to reduce the T_1 sensitivity while keeping TR short: the flip angle can be reduced (Buxton *et al.* 1987). At first glance, this would seem to reduce just M_T (and thus the signal) by tipping only a part of the longitudinal magnetization into the transverse plane. But this also modifies the steady-state amplitude of the longitudinal magnetization in a way that reduces the sensitivity to T_1. Consider the steady-state signal generated when TR is much smaller than T_1. For a 90° pulse, the recovery during TR is very small, and so the signal is weak (often described as saturated). If the flip angle is small, however, the longitudinal magnetization is hardly disturbed by the RF pulse. As a result, there is very little relaxation to do; the longitudinal magnetization is already near its equilibrium value. The sensitivity of the resulting signal to differences in T_1 is then greatly reduced. In summary, for short TR, the signal is T_1 weighted for large flip angles but only proton density weighted for small flip angles. Figure 3.9 illustrates how the tissue contrast in an image can be manipulated by adjusting the flip angle.

The decay T_2^*

The simple GRE pulse sequence described above illustrates how pulse sequence parameters and intrinsic tissue parameters interact to produce the MR signal. But one important tissue parameter, T_2, did not enter into the discussion. The reason T_2 was left out was that we assumed that the signal was measured immediately after the RF pulse. However, the GRE sequence can be modified to insert a delay after the RF pulse before data acquisition begins. During this delay, M_T and thus the signal, would be expected to decrease exponentially with a time constant T_2 through transverse relaxation. If we performed this experiment, we would indeed find that the signal decreased, but typically by much more than we would expect for a known T_2. This enhanced decay is described in terms of an *apparent transverse relaxation time* T_2^* (read as "T_2 star") that is smaller than T_2.

The source of this T_2^* effect is magnetic field inhomogeneity. Because the precession frequency of the local M_T is proportional to the local magnetic field, any field inhomogeneity will lead to a range of precession rates. Over time, the precessing magnetization vectors will get out of phase with one another so that they no longer add coherently to form the net magnetization. As a result, the net signal is reduced because of this destructive interference. At first glance this seems similar to the argument for T_2 relaxation itself. It was argued above that the net value of M_T would decrease over time because each spin feels a random fluctuating magnetic field in addition to B_0. Because each spin feels a different pattern of fluctuating fields, the spins gradually become out of phase with one another (the phase dispersion increases) and net M_T is reduced. The T_2^* effect, however, results from constant field offsets rather than fluctuating fields. Because these field offsets are static, there is a clever way to correct for these inhomogeneity effects.

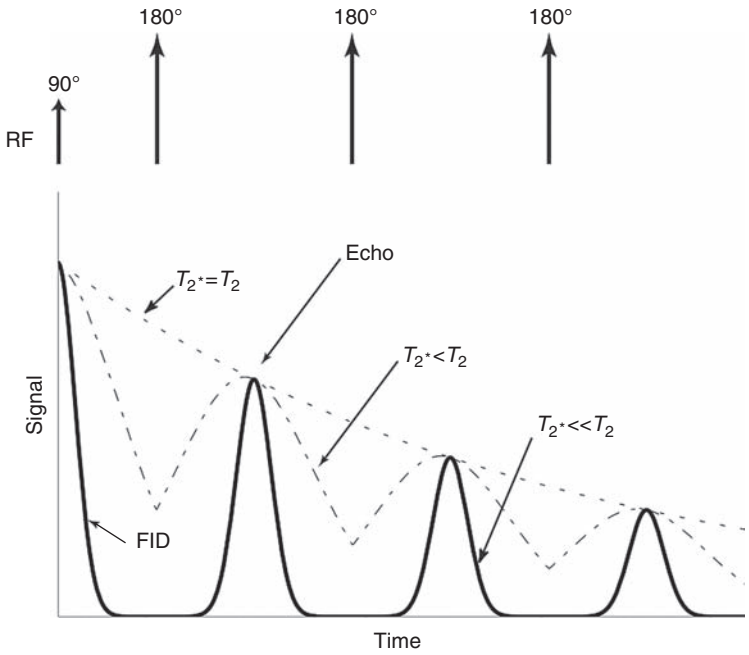

Fig. 3.10. Spin echo (SE). In an inhomogeneous field, spins precess at different rates, and the Free induction decay (FID) signal created after a 90° excitation pulse decays with a time constant T_2^* that is less than T_2. A 180° radiofrequency (RF) pulse refocuses this signal loss owing to static field offsets and creates a transient SE. The SE signal decays with the true T_2 of the sample. Repeated 180° pulses generate repeated SEs.

Spin echoes

In 1950, Hahn showed that a remarkable phenomenon occurs when a second RF pulse is applied following a delay after the first RF pulse. After the first RF pulse, an FID signal is generated that decays away quickly because of a short T_2^*. A second RF pulse applied after a delay TE/2 creates an echo (a *spin echo* [SE]) of the original FID signal at a time TE, the *echo time*. This effect can be quite dramatic. The original FID signal can be reduced to an undetectable level, but the second pulse will create a strong echo. However, the echo is reduced in intensity from the original full FID by true T_2 decay. As soon as the echo forms, it will again decay quickly through T_2^* effects, but another RF pulse will create another echo. This can be carried on indefinitely, but each echo is weaker than the last because of T_2 decay (Fig. 3.10).

The phenomenon of echo formation from a second RF pulse is very general and occurs for any flip angle, although for small flip angles the echo is weak. Hahn's original demonstration (1950) used 90° flip angles, but in most applications a 180° pulse is used because it creates the strongest echo. The effect of a 180° pulse is illustrated in Fig. 3.11. After the initial 90° pulse, the individual magnetization vectors corresponding to different parts of the sample are in-phase and so add coherently. Owing to field inhomogeneity, however, each precesses at a slightly different rate. The growing phase dispersion can be visualized by imagining that we ourselves are precessing at the average rate. That is, we plot how these vectors evolve in time in a *rotating reference frame* rotating at the average precession rate. Then a magnetization vector precessing at precisely the average rate appears stationary, whereas vectors precessing faster rotate in one direction and vectors precessing more slowly rotate in the other direction.

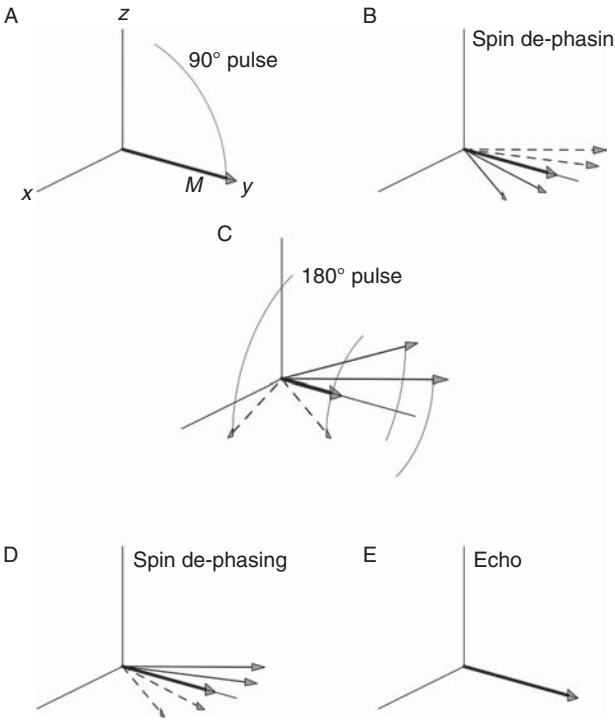

Fig. 3.11. Formation of a spin echo. After tipping the magnetization into the transverse plane (A), spins in different fields precess at different rates (B). Individual magnetization vectors begin to fan out, reducing the net signal. The 180° pulse at a time TE/2 flips the transverse plane like a pancake (C), and each magnetization vector continues to precess in the same direction (D), so that they realign to form a spin echo at TE (E). TE, echo time.

Over time, the vectors spread into a fan in the transverse plane, and the net signal is reduced. However, if we now apply a 180° RF pulse, the fan of vectors is rotated through 180°, so that whatever phase was acquired by a particular vector is converted into a negative phase. After the 180° pulse, each vector will again precess at the same rate as before. At TE, each spin will have acquired the same additional phase that it acquired during the interval TE/2 between the 90° and 180° pulses, and the net acquired phase is thus precisely zero. That is, all vectors come back in-phase and create an echo.

This effect works because the phase accumulated by a particular vector is simply proportional to elapsed time, so that the phase acquired during the first half of the echo time is identical to that acquired during the second half. Because the 180° pulse reverses the sign of the phase halfway through, the net phase for each vector is zero at the echo time. Because of this effect, a 180° RF pulse is often called a *refocusing pulse*. However, a 180° pulse does not refocus true T_2 effects because the additional phase acquired from random fluctuations is not the same in the first and second halves of the TE. A multi-echo pulse sequence using a string of 180° pulses thus will create a chain of echoes with the peak of each echo falling on the true T_2 exponential decay curve.

Spin echo pulse sequence

The *SE pulse sequence* is the workhorse of clinical MRI. Field inhomogeneity is difficult to eliminate, particularly because the head itself is inhomogeneous, and T_2* effects lead to signal loss in areas near air–tissue and bone–tissue interfaces (discussed in more detail later in the book). The particular advantage of the SE pulse sequence is that it is insensitive to these inhomogeneities, so the local signal and the tissue contrast reflect only the interaction of the

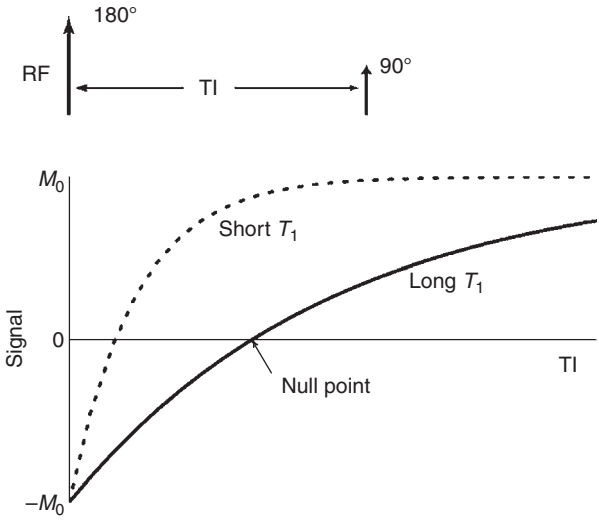

Fig. 3.12. Inversion recovery (IR). In an IR pulse sequence, an initial 180° inversion pulse flips the magnetization from $+z$ to $-z$, and it then relaxes back toward equilibrium (M_0). After an inversion time TI, a 90° excitation pulse tips the current longitudinal magnetization into the transverse plane to generate a signal. The signal is strongly T_1 weighted, and for a particular value of TI exhibits a null point where no signal is generated because the longitudinal magnetization is passing through zero.

pulse sequence parameters with the intrinsic tissue parameters. The SE sequence is nearly always used with a 90°–180° combination of RF pulses, so the flip angles usually are not adjusted to control image contrast. That leaves TR and TE as the adjustable pulse sequence parameters, and three tissue parameters affect the signal: M_0, T_1, and T_2. The dependence of the SE signal on proton density and T_1 is similar to that of the GRE sequence with a 90° pulse. The dependence on T_2 is simply an exponential decrease of the signal with increasing TE. When TE is much shorter than T_2, there is little decay, so the signal is insensitive to T_2. For TE $\gg T_2$, there is substantial decay and, therefore, very little signal left to measure. When TE is comparable to T_2, the signal is strongly sensitive to the local T_2, and the signal is described as T_2 weighted.

In an SE pulse sequence, the signal is measured at the peak of the echo, where the effects of field inhomogeneities are refocused, and this is the standard implementation for clinical imaging. In applications such as fMRI, however, which are based on the BOLD effect, the microscopic field variations induced by changes in blood oxygenation make the MR signal sensitive to brain activation. Some sensitivity to field variations can be retained by shifting the time of data collection away from the echo peak. In such an *asymmetric spin echo pulse sequence*, the data acquisition occurs at a fixed time τ after the RF pulse, but the time of the 180° pulse is shifted so that the SE occurs at a time TE different from τ. Then, in addition to T_2 decay for a time t, there will also be an additional decay owing to the phase dispersion resulting from evolution in the inhomogeneous field for a time $\tau - \text{TE}$.

Inversion recovery pulse sequence

A third widely used pulse sequence is called *inversion recovery* (IR), illustrated in Fig. 3.12. This sequence begins with a 180° pulse, then after a delay (called the *inversion time* [TI]), a regular SE or GRE pulse sequence is started. The initial 180° pulse is called an inversion pulse and can be thought of as a preparation pulse that affects the longitudinal magnetization before it is tipped over to generate a signal. For the IR sequence, the preparation pulse enhances the T_1 weighting of the signal. The effect of the initial 180° pulse is to invert the longitudinal magnetization so that it points along the $-z$ axis instead of $+z$. Note that this

does not yet create a signal, because there is no M_T. After the inversion pulse, the longitudinal magnetization begins to re-grow toward its equilibrium value along $+z$. After a delay of TI a 90° pulse is applied; this pulse tips whatever longitudinal magnetization exists at that time into the transverse plane. The resulting signal thus reflects the degree of recovery during the time TI.

If TI is much longer than T_1, the longitudinal magnetization recovers completely, and the inversion has no effect on the resulting signal. But if TI is comparable to T_1, the recovery is incomplete, and the signal is strongly T_1 weighted. The T_1 weighting is more pronounced than in a typical T_1-weighted GRE or SE pulse sequence because the longitudinal magnetization is recovering over a wider dynamic range, from $-M_0$ to M_0 instead of from 0 to M_0. This is the essential difference between an IR experiment (following a 180° pulse) and a saturation recovery experiment (following a 90° pulse). Indeed, because the longitudinal magnetization in an IR experiment is recovering from a negative value to a positive value, there is a particular value of TI, called the *null point*, when the longitudinal magnetization is zero, and for this TI no signal is generated. A typical set of parameters for T_1-weighted IR is TI approximately equal to T_1 and TR several times longer than T_1 to allow recovery before the pulse sequence is repeated, beginning with another inversion pulse.

The SE and IR pulse sequences illustrate two different uses of a 180° RF pulse, as reflected in the descriptive terms: it is a "refocusing" pulse in the SE sequence and an "inversion" pulse in the IR sequence. In both cases, it is the same RF pulse. The difference is whether we are concerned with its effect on M_T or on longitudinal magnetization. A 180° pulse flips M_T like a pancake, reversing the phase of the M_T and producing an echo, but the same flip sends the longitudinal magnetization from $+z$ to $-z$. In the SE experiment, the inversion effect of the 180° pulse is small because the longitudinal magnetization was reduced to zero by the initial 90° pulse, so it has only recovered a small amount during the time TE/2 between the 90° and 180° pulses. In the IR experiment, there is no M_T to refocus at the time of the 180° pulse, and we are interested only in its inversion effect on the longitudinal magnetization.

References

Bloch F (1953) The principle of nuclear induction. *Science* **118**:425–430

Bloch F, Hansen WW, Packard M (1946) Nuclear induction. *Phys Rev* **69**:127

Buxton RB, Edelman RR, Rosen BR, Wismer GL, Brady TJ (1987) Contrast in rapid MR imaging: T1- and T2-weighted imaging. *J Comput Assist Tomogr* **11**:7–16

Hahn EL (1950) Spin echoes. *Phys Rev* **80**:580–593

Kwong KK, Belliveau JW, Chesler DA, *et al.* (1992) Dynamic magnetic resonance imaging of human brain activity during primary sensory stimulation. *Proc Natl Acad Sci USA* **89**:5675–5679

Lauterbur PC (1973) Image formation by induced local interactions: examples employing nuclear magnetic resonance. *Nature* **242**:190–191

Mansfield P (1977) Multi-planar image formation using NMR spin echoes. *J Phys* **C 10**:L55–L58

Ogawa S, Lee TM, Nayak AS, Glynn P (1990) Oxygenation-sensitive contrast in magnetic resonance image of rodent brain at high magnetic fields. *Magn Reson Med* **14**:68–78

Purcell EM (1953) Research in nuclear magnetism. *Science* **118**:431–436

Purcell EM, Torrey HC, Pound RV (1946) Resonance absorption by nuclear magnetic moments in a solid. *Phys Rev* **69**: 37

Vleck JHV (1970) A third of a century of paramagnetic relaxation and resonance. In *International Symposium on Electron and Nuclear Magnetic Resonance*, Coogan CK, Ham NS, Stuart SN *et al.*, eds. Melbourne: Plenum Press, pp. 1–10